Association Behavior of Poly(methacrylic acid)-*block*-poly(methyl methacrylate) in Aqueous Medium: Potentiometric and Laser Light Scattering Studies

P. Ravi,[†] C. Wang,[†] K. C. Tam,*[,†] and L. H. Gan[‡]

Singapore-MIT Alliance, School of Mechanical and Production Engineering, Natural Sciences, National Institute of Education, Nanyang Technological University, 50 Nanyang Avenue, Singapore 639798

Received August 12, 2002; Revised Manuscript Received October 17, 2002

ABSTRACT: The atom transfer radical polymerization technique was used to synthesize poly(methacrylic acid-*block*-methyl methacrylate) ($P(MAA_{102}$-*b*-$MMA_{10})$) copolymer in order to study the aggregation behavior in aqueous solution over the course of neutralization. A combination of static and dynamic light scattering (SLS, DLS) and potentiometric titration techniques were used to investigate the size and shape of the micelle at various degrees of neutralization. The hydrodynamic radius (R_h) determined from dynamic light scattering increases from ∼26 nm (for unneutralized) to ∼42 nm (for completely neutralized sample). Both potentiometric and laser light scattering studies indicate the formation of a core−shell micelle. The weighted average molecular weights of the polymer and micelle are 1.18×10^4 and 2.25×10^5 g/mol, respectively, which suggests that the aggregation number of the micelle is ∼20.

Introduction

In recent years, much interest has been focused on the self-assembled structure of polyelectrolyte amphiphilic block copolymers in aqueous solution due to its many important applications such as thickeners, coatings, drug delivery systems, nanoparticles, and nanoreactors.[1−3] It has been shown that these types of block copolymers can also be used as polymeric surfactants to stabilize dispersions.[4] The characteristics of these polymers are to respond to external stimuli such as pH or temperature, which makes them useful for specific applications.[5,6] The outstanding feature of amphiphilic block copolymers is that they self-assemble to form micelles with well-defined size and shape. The size and shape of the micelle not only depend on the chain length but also depend on the balance between hydrophobic and hydrophilic segments. For pH-sensitive systems, the size, shape, and thermodynamics depend on the degree of neutralization. By varying the block lengths or adjusting the pH and ionic strength of the solution, one can control the size and the aggregation number of the micelle.[7]

Systematic studies on the polyelectrolyte amphiphilic block copolymers of poly(styrene-*b*-acrylic acid) with respect to micellar size and structure have been reported.[8,9] Schuch et al. proposed the formation of small vesicle-like structure from poly(isobutylene)-*b*-poly(methacrylic acid) in aqueous medium.[10] Hybrid polymeric micelles with compact polystyrene cores and mixed poly(methacrylic acid)/poly(ethylene oxide) shells in 1,4-dioxane(80 vol %)/water have been reported by Stepanec and co-workers.[11] The formation of three-layer micelles from pH-responsive triblock ((polystyrene-*b*-poly(2-vinylpyridine)-*b*-poly(ethylene oxide)) copolymer in water was studied by Gohy et al.[12] and Kriz et al.[13] It has been demonstrated that the pH-sensitive poly(2-vinylpyridine) shell can be used to tune the size of the vesicle. This effect was mainly attributed to electrostatic repulsion between the charged polyelectrolyte chains. Talingting et al.[14] observed onion-type micelles form polyelectrolytes based on polystyrene-*block*-poly(2-vinylpyridine) and poly(2-vinylpyridine)-*block*-poly(ethylene oxide) systems. Extensive research has been carried out by Tuzar and co-workers on poly(methyl methacrylate)-*block*-poly(acrylic acid)-based polyelectrolytes in aqueous solution.[15] Liu et al. have used poly(methacrylic acid)-*b*-poly(methyl methacrylate) [P(MAA-*b*-MMA)] copolymer as dispersants for microemulsion polymerization.[16] The radical polymerization of methyl methacrylate at the core−shell interface of polystyrene-*block*-poly(methacrylic acid) micelles was examined by Tuzar and co-workers using the NMR technique.[17] Tuzar and co-workers also reported fluorescence studies of amphiphilic poly(methacrylic acid)-*block*-polystyrene-*block*-poly(methacrylic acid) micelles, where they observed a significant fraction (ca. 20−30%) of the pyrene molecules on or near the polystyrene−water interface, and the diffusion of the probe out of the micelle is the rate-determining step in the release and exchange of large hydrophobes.[18]

However, detailed studies with respect to shape and size of the micelle of P(MAA-*b*-MMA) polymer having short hydrophobic segments as a function of degree of neutralization have not been reported. The objective of this paper is to investigate the association behavior (for e.g. critical micellar concentration and aggregation number) of P(MAA-*b*-MMA) over the course of neutralization, where such information is currently not available.

Experimental Section

Materials. *tert*-Butyl methacrylate (tBMA, Aldrich, 98%) was passed through a basic alumina column, stirred over CaH_2, and distilled under reduced pressure. Methyl methacrylate (MMA, Aldrich, 98%) was stirred over CaH_2 and distilled under vacuum. CuBr (99.99%), $CuBr_2$, CuCl (99.98%,), *N*,*N*,*N*′,*N*″,*N*″-pentamethyldiethylenetriamine (PMDETA),

[†] Singapore-MIT Alliance, School of Mechanical and Production Engineering.
[‡] Natural Sciences, National Institute of Education.
* Corresponding author: e-mail mkctam@ntu.edu.sg.

10.1021/ma021302j CCC: $25.00
Published on Web 12/14/2002

methyl 2-bromopropionate, anisole, and diphenyl ether were purchased from Aldrich and used without further purification.

Synthesis of Poly(*tert*-butyl methacrylate) (P(tBMA)) Macroinitiator. All synthetic steps were carried out under an argon atmosphere. In a typical experiment, CuBr, $CuBr_2$, and a magnetic bar were introduced into a predried Schlenk flask and tightly sealed with rubber septum. Deoxygenated acetone (25 vol % with respect to monomer) followed by the monomer and PMDETA was introduced into the flask via an Ar-washed syringe and stirred until the system became homogeneous. Three "freeze−pump−thaw" cycles were performed to remove any oxygen from the polymerization solution. Finally, degassed initiator was introduced using Ar purged syringe and placed in a thermostated oil bath at 60 °C. As soon as the initiator was added, the system turned dark green, indicating the progress of the polymerization. After 80 min, the polymer was isolated by dissolving in tetrahydrofuran (THF) and passing through alumina column to remove the catalyst. Finally, the polymer was recovered by precipitating into 10-fold excess of water/methanol (1:1) mixture, filtered, and dried under vacuum to constant weight. Yield = 86%. M_n = 12 871 Da and M_w/M_n = 1.28.

Purification of Macroinitiator. The macroinitiator was dissolved in acetone and stirred with DOWEX MSC macroporous ion-exange resin for about 1 h, and the solution was filtered by passing through an alumina column. Finally, the solvent was partially removed by rotary evaporation and precipitated into 10-fold excess of a water/methanol (50:50) mixture. The solid was filtered and dried under vacuum.

Synthesis of P(tBMA-*b*-MMA) Copolymer. A known amount of Br-terminated P(tBMA) as a macroinitiator and CuCl were added into a Schlenk flask and dissolved in a minimum amount of degassed toluene. Monomer and diphenyl ether (equal amount to monomer) were introduced using Ar washed syringe. The reaction mixture was degassed three times using freeze−pump−thaw cycles. Finally, degassed ligand (PMDETA) was introduced using Ar-purged syringe, and the flask was placed in an oil bath, which was thermostated at 90 °C. After the reaction was completed, the catalyst was removed by passing through an alumina column, and the polymer was recovered by reprecipitation in cold methanol. The number-average molecular weight M_n = 15 543 Da and M_w/M_n = 1.20. Subsequently, the *tert*-butyl groups of the P(tBMA) block were hydrolyzed with concentrated hydrochloric acid in dioxane at 85 °C for 6 h to form a PMAA blocks. FT-IR (KBr pellet) showed a broad peak at 3500 cm^{-1}, which is the characteristic absorption for carboxylic acid, and the content of the acid was quantified by potentiometric titration.

Polymer Characterization. *Gel Permeation Chromatography.* Polymer molecular weights and molecular weight distributions were determined using gel permeation chromatography (GPC). An Agilent 1100 series GPC system equipped with a LC pump, PLgel 5 μm MIXED-C column, and RI detector was used. The column was calibrated with narrow molecular weight polystyrene standards. HPLC grade THF stabilized with BHT was used as a mobile phase. The flow rate was maintained at 1.0 mL min^{-1}.

Nuclear Magnetic Resonance Spectroscopy (NMR). The ^{1}H NMR spectrum for the precursor block copolymer was measured using a Brüker DRX400 instrument in $CDCl_3$. The ^{1}H NMR spectrum of the block copolymer allows the molar composition to be determined from the relative intensity at 1.42 ppm ($-C(C\boldsymbol{H}_3)_3$ of the tBMA block) and 3.69 ppm ($-OC\boldsymbol{H}_3$ of MMA block).

Preparation of P(MAA-*b*-MMA) Polymer Solution. The P(MAA-*b*-MMA) block copolymer at low pH (i.e., ∼3) is insoluble in aqueous medium. Therefore, the polymer was dissolved titrating 1 M NaOH solution until the number of moles of NaOH is equivalent to the carboxylic groups in the polymer. The polymer solution was continuously stirred for 1−2 h, until the solution became homogeneous. Thereafter, the polymer solution was neutralized with the addition of 1 M HCl until pH of ∼3, and the polymer solution remained homogeneous and transparent.

Potentiometric Titration. An ABU93 Triburette titration system equipped with Radiometer pHG201 pH glass and Radiometer REF201 reference electrodes was used to conduct the potentiometric titrations. All the titrations were performed under constant stirring at 25 °C in a titration vessel filled with 100 mL of 0.1 wt % P(MAA-*b*-MMA) polymer solution. A 1 M standard NaOH solution (from Merck) was used. Forty seconds of lag time was allowed between two dosages to ensure that the reaction has reached equilibrium.

Laser Light Scattering. The laser light scattering experiments were conducted using the Brookhaven laser light scattering system. This system consists of a BI200SM goniometer, a BI-9000AT digital correlator, and other supporting data acquisition and analysis software and accessories. An argon ion vertically polarized 488 nm laser was used as the light source. In DLS, the time correlation function of the scattered intensity $G_2(t)$, which is defined as $G_2(t) = I(t)I(t + \Delta t)$ where $I(t)$ is the intensity at time t and Δt is the lag time, was analyzed using the inverse Laplace transformation technique (REPES, in our case) to produce the distribution function of decay times. The concentration of the polymer solutions investigated by light scattering is 0.02 wt %, which is in the dilute solution regime where the behavior of individual particles can be characterized. Several measurements were performed at varying scattering angles for a given sample to obtain an average hydrodynamic radius. The variation in the R_h values was found to be small.

Results and Discussion

Polymer Synthesis. Though the polymerization of tBMA by ATRP technique has previously been reported,[19] block copolymerization with MMA has not been studied. In the earlier report, tBMA was polymerized using ethyl 2-bromoisobutyrate as an initiator along with CuCl as a catalyst.[19] The resulting homopolymer contains a mixture of both −Cl and −Br end groups. Using tBMA as a macroinitiator to block copolymerize with MMA may result in the broadening of the molecular weight distribution due to difference in the initiation rates. In addition, it has been reported that Cl end groups are poor initiator for the MMA monomer.[20] Bearing this in mind, we synthesized P(tBMA)−Br using CuBr as a catalyst, similar to that reported by Davis et al. for *tert*-butyl acrylate.[21] Using this technique, we achieved a polydispersity of 1.28 for the macromonomer. Interestingly, subsequent copolymerization with MMA produced a block copolymer with similar narrow molar mass distribution of M_w/M_n = 1.20 with 65% yield. The slight decrease in the polydispersity may be due to the removal of lower MW fragments as they were more soluble in cold methanol. The block lengths of the copolymer calculated from the ^{1}H NMR spectrum (Figure 1) were 102 and 10 for tBMA and MMA, respectively.

Potentiometric and Conductometric Titration. The degree of neutralization, α, of the carboxyl group is defined by the equation

$$\alpha = \frac{[\mathrm{BASE}] + [\mathrm{H^+}] - [\mathrm{OH^-}]}{C_{\mathrm{COOH}}} \qquad (1)$$

where [BASE], $[H^+]$, and $[OH^-]$ are the molarities of added base, free hydrogen ion, and hydroxide ion, respectively, and C_{COOH} is the total concentration of methacrylic acid groups expressed in mol/L. The $[H^+]$ and $[OH^-]$ ions were obtained from the pH values assuming the activity coefficient is unity. With this definition, α = 1 at complete neutralization. Figure 2 shows the pH curves plotted against α obtained from

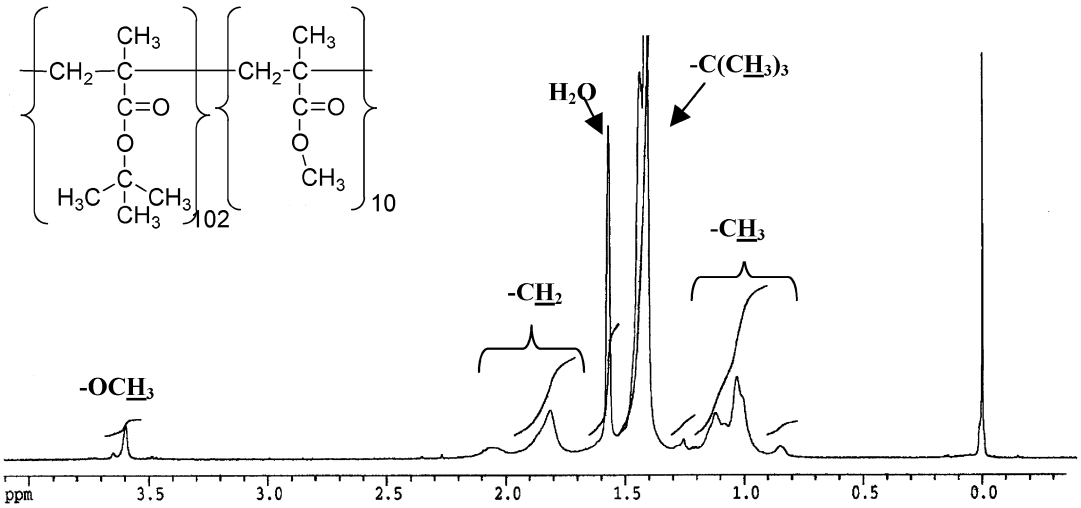

Figure 1. ^{1}H NMR spectrum of P(tBMA-*b*-MMA) block copolymer in $CDCl_3$ at 298 K.

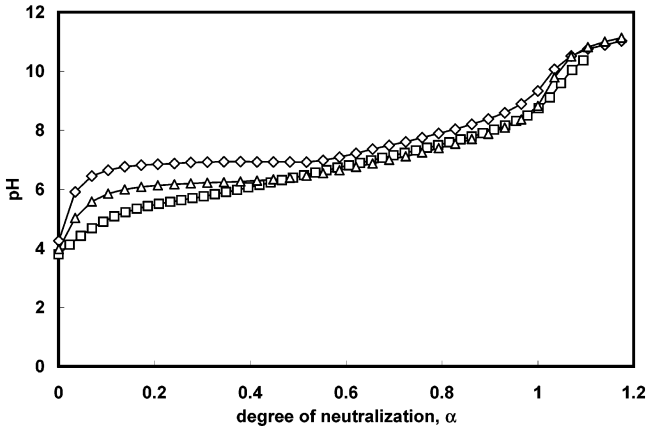

Figure 2. Dependence of pH on α for 0.1 wt % polymer solutions: (□) P(MAA-*b*-MMA) block coplolymer; (◇) MAA−EA random copolymer without solublization; (△) MAA−EA random copolymer with solublization.

titrating 1 M NaOH into 0.1 wt % aqueous solution of the P(MAA-*b*-MMA) polymer and the random MAA−EA (MAA−EA in equal molar ratio) copolymers. Since we are interested in the behavior of the acid groups, the effect of EA or MMA is not considered here. The curve designated as pH-1 (open diamonds) characterizes the titration where the MAA−EA polymer was titrated with NaOH directly, whereas the curve indicated as pH-2 (open triangles) characterizes the titration where the MAA−EA polymer was prepared through a solubilization step that is identical to the P(MAA-*b*-MMA) block copolymer. Both curves (pH-1 and pH-2) exhibit a plateau in the range of α of 0.1−0.5, which suggests a two-step dissociation and a conformational transition of the polymer.[22,23] The reason for the pH-2 curve being lower than pH-1 is due to the presence of smaller colloidal particles and excess NaCl introduced during the neutralization process, which favors the dissociation of the carboxylic groups.[23] On the other hand, the pH corresponding to the titration of the P(MAA-*b*-MMA) block copolymer (open squares) increases gradually with α over the entire course of neutralization. This monotonic dependence of pH on α may suggest that the P(MAA-*b*-MMA) polymer dissociates in one step, and the conformation of the polymer particles does not change significantly during the process of neutralization.

The negative logarithm dissociation constant (pK_a) vs neutralization degree (α) curve is more informative. The pK_a is expressed by the Henderson−Hasselbalch equation

$$pK_a \equiv pH + \log \frac{1-\alpha}{\alpha} \tag{2}$$

By extrapolating the pK_a curve to zero degree of neutralization, the negative logarithm of the intrinsic dissociation constant pK_0 can be determined. It is known that the intrinsic dissociation constant, K_0, is related to the standard change of the free energy (ΔG_0) for the dissociation of H^+ from an isolated acid group, whereas the apparent dissociation constant, K_a, contains an additional contribution, ΔG_{el}, which is related to the extra work to overcome the electrostatic attraction between the H^+ and ∼COO^- when transferring the proton from the polyanion to the bulk.[24−26] Thus, pK_a can be written as a sum of two terms:

$$pK_a = pK_0 + 0.4343 \frac{dG_{el}}{RT\, d\alpha} \tag{3}$$

where R is the gas constant and T is the absolute temperature. ΔG_{el} (from $\alpha = 0$ to 1) can be calculated from the graphical integration of the extended Henderson−Haselbalch equation:[27−30]

$$\Delta G_{el} = 2.30RT\int_0^1 [pK_{(\alpha)} - pK_0]\, d\alpha \tag{4}$$

The pK_a curves of P(MAA-*b*-MMA) polymer (open squares) and random MAA−EA copolymer are shown in Figure 3. Similarly, the pK_a-1 curve (open diamonds) represents the titration without solublization step, whereas the pK_a-2 curve (open triangles) represents the titration where the polymer was solublized prior to the measurements. The pK_a curves (pK_a-1 and pK_a-2) of the random MAA−EA copolymer exhibit a negative slope between two inflection points in the range of α from 0.1 to 0.5, which corresponds to the plateau region shown on the pH curves (Figure 2). This feature is attributed to the discontinuous conformational transition of polymer particles in the course of neutralization.[22,23] The polymer expands initially from insoluble latex particle to swollen hydrated random particles driven by the electrostatic repulsion between the negatively charged

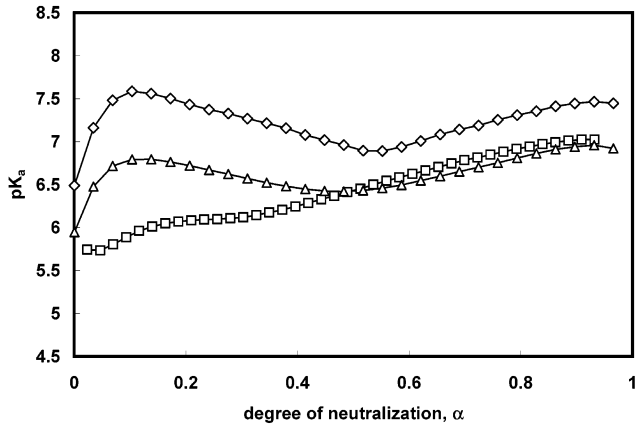

Figure 3. Dependence of pK_a on α for 0.1 wt % polymer solutions: (□) P(MAA-*b*-MMA) block coplolymer; (◇) MAA−EA random copolymer without solublization; (△) MAA−EA random copolymer with solublization.

carboxylate groups. Thereafter, the swollen particles disintegrate into several smaller clusters when the electrostatic repulsion exceeds the hydrophobic attraction between the EA groups. Moreover, the conformational change that unfolds and expands the compact latex particle is favorable for the dissociation of protons from the polyanions, which is reflected by the negative slope observed in the pK_a curve.[22,23] It should be noted that the disintegration of the swollen particle may be absent for the polymer prepared through solublization since the insoluble latex particles are already disintegrated and stabilized in the process of solublization. However, the plateau region and the negative slope shown on the pH-2 and pK_a-2 curves indicate that the conformational transition is still present during neutralization, and this conformational change represents the expansion of the polymer particles. The values of ΔG_{el} determined from the area under the pK_a curve are 4.27 and 3.99 kJ/mol for pK_a-1 and pK_a-2, respectively. This is attributed to the presence of salt introduced by the solublization, which favors the dissociation of the carboxylic groups, and to the lower energy required to deprontonate the less compact and relatively smaller polymer particles.[23]

It is interesting to compare the pK_a curve of P(MAA-*b*-MMA) (open squares) copolymer with pK_a-2 (open triangles) curve. The pK_a curve of the block copolymer exhibits a steady increase with α, which is similar to poly(acrylic acid) and poly(2-methylengeglutaric acid). The pK_a value increases in the α range from 0 to ∼0.2 and levels off from α ∼ 0.15 to ∼0.3; thereafter, it increases again until it reaches the fully neutralization (α = 1) stage. As shown in Figure 3, the pK_a curves of the block and random copolymers are remarkably different, despite the fact that they contain identical acid content (MAA). The continuous increase of pK_a of the P(MAA-*b*-MMA) polymer suggests that it is more difficult to extract H^+ from ∼COOH due to the proton−polyanion electrostatic attraction as the polymer is progressively being neutralized. It implies that the P(MAA-*b*-MMA) copolymer may exist as a core−shell micelle, where the MMA segments of the polymer chains aggregate to form a hydrophobic core, accompanied by a shell consisting of the hydrophilic MAA segments. The addition of NaOH neutralizes and ionizes the carboxylic groups of the shell layer, which increases the electrostatic potential on the micellar surface. Thus, the Coulombic attraction between H^+ and ∼COO^- is enhanced, which is unfavorable for the dissociation of the carboxylic groups. The shell layer may expand to a certain extent, driven by the electrostatic repulsion between the charged carboxylate groups, as reflected by the plateau region at α = 0.14−0.30. However, the electrostatic repulsive force is not strong enough to overcome the hydrophobic attractive force of the MMA core; thus, the conformation of the polymer and the micelle structure remains unchanged. This hypothesis is furthermore confirmed by the light scattering studies, which will be discussed later, and the proposed core−shell structure of the micelle is shown in Figure 9.

By extrapolating the pK_a curves to zero degree of neutralization, the pK_0 values were determined to be 5.6 and 5.9 for block and random copolymers, respectively. The reasonably good agreement of the pK_0 values for the block and random copolymers suggests that the spontaneous dissociation of the carboxylic group and the standard free energy change (ΔG_0) are mainly dependent on the environment of the protons. By performing graphical integration using eq 4, values of ΔG_{el} were calculated to be 2.39 and 3.99 kJ/mol for block and random copolymers, respectively. Compared to the random MAA−EA copolymer, the dissociation of the P(MAA-*b*-MMA) polymer is relatively easier, and less work is required to extract the proton from the polyanion during neutralization. The difference in the ΔG_{el} between the block and random copolymers may be attributed to the different structures of the two polymer systems in solution. For the block copolymer, acid groups are distributed on the shell layer of the micelle and are accessible to the base; thus, it is more favorable for dissociation. However, for the random copolymer, some of the carboxylic groups are trapped inside the compact particles and are not readily accessible to the base; thus, more work is required.

Dynamic Light Scattering. Dynamic and static light scattering were used to measure the particle size of the P(MAA-*b*-MMA) polymer at different degree of neutralization. Figure 4a shows a typical autocorrelation function $C(t)$ obtained from DLS at scattering angle of 90° together with the relaxation time (τ) distribution function determined by the REPES analysis of this autocorrelation function. The relaxation time distribution functions for the polymer solutions at different α were plotted in Figure 4b. Each of the distribution functions is unimodal. The relaxation time increases until α reaches 0.3, reflecting the gradual expansion of the shell layer of micelles driven by the electrostatic repulsion between ionized carboxylate groups. Thereafter, the relaxation time remains essentially constant. Figure 5 shows the relaxation time distribution functions of fully neutralized 0.02 wt % P(MAA-*b*-MMA) polymer solution measured at different scattering angles. The distribution function is unimodal, and it shifts to lower relaxation time with increasing scattering angles. The decay rate Γ was plotted against q^2 as shown in Figure 6. Γ exhibits a good linear relationship with q^2, which confirms that the distribution function is caused by the translational diffusion of the polymer micelles.

The apparent hydrodynamic radius was determined from the Stokes−Einstein equation:

$$R_h = \frac{kTq^2}{6\pi\eta\Gamma} \tag{5}$$

where k is the Boltzmann constant, q is the scattering vector [$q = (4\pi n \sin(\theta/2))/\lambda$, where n is the refractive

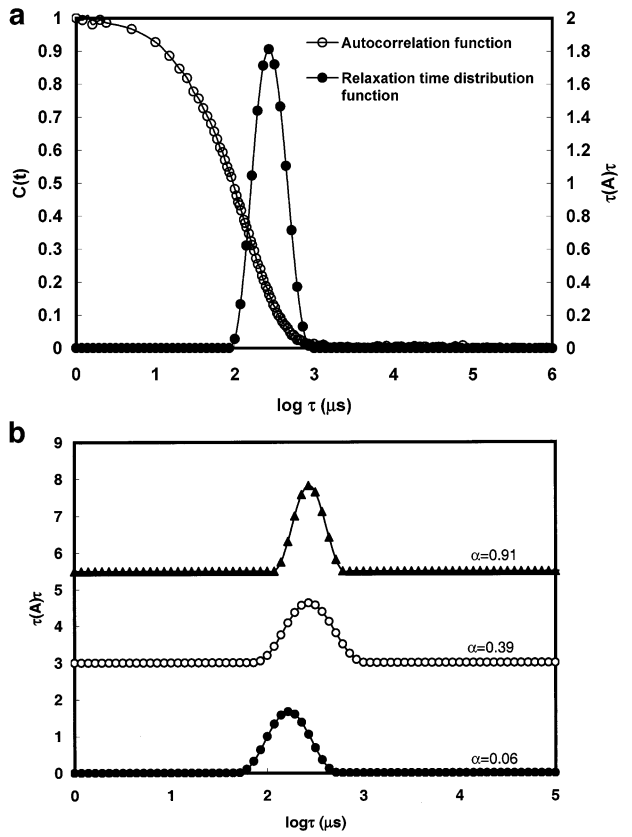

Figure 4. (a**)** Autocorrelation and relaxation time distribution functions obtained from DLS for 0.02 wt % P(MAA-*b*-MMA) polymer solution at $\alpha = 0.46$. (b) Characteristic relaxation time (micelle center-of-mass diffusion) distribution functions obtained from DLS for 0.02 wt % P(MAA-*b*-MMA) polymer solution at different degree of neutralization.

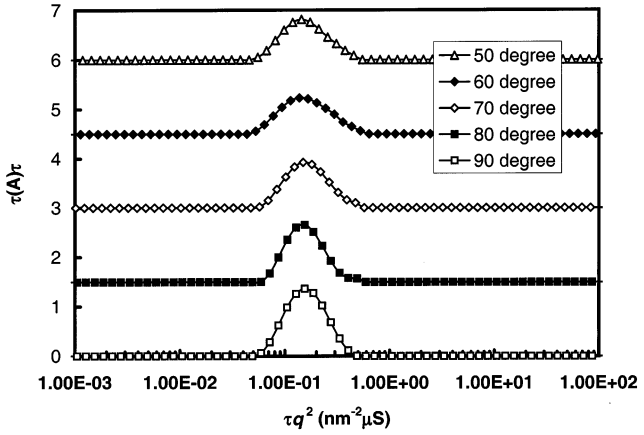

Figure 5. Distribution functions for 0.02 wt % fully neutralized P(MAA-*b*-MMA) polymer solution at different scattering angles: (●) 90°; (◇) 80°; (△) 70°; (○) 60°; (□) 50°.

index of the solution, θ is the scattering angle, and λ is the wavelength of the incident laser light in a vacuum], η is the solvent viscosity, and Γ is the decay rate. The values of hydrodynamic radius (R_h^{app}) over the process of neutralization are plotted against α in Figure 7. The R_h^{app} of the unneutralized micelle is 26 nm. With the increase in degree of neutralization, the micelle swells due to the ionization of MAA segments and the R_h^{app} increases with α, approaching a maximum of ~45 nm at $\alpha \sim 0.3$. Thereafter it levels off and then decreases slightly to a constant value of ~42 nm at α greater than 0.6. By comparing Figure 7 with Figure 3, it is evident that the micelle swells over the same α range (from ~0.1 to ~0.3) where the pK_a curve flattens, which confirms that the plateau on the pK_a curve characterizes the expansion of the micelle upon the electrostatic repulsion of ionized MAA groups. The slight decrease of R_h^{app} at $\alpha \sim 0.6$ may result from counterion condensation on the surface of the micelles when the charge density is sufficiently high, which screens the electrostatic repulsion between carboxylate groups and hence the micelle shrinks slightly.

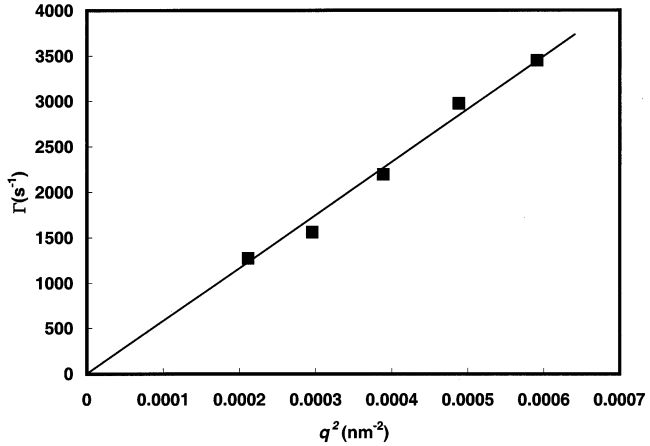

Figure 6. Dependence of the decay rate Γ on the square of the scattering vector (q^2).

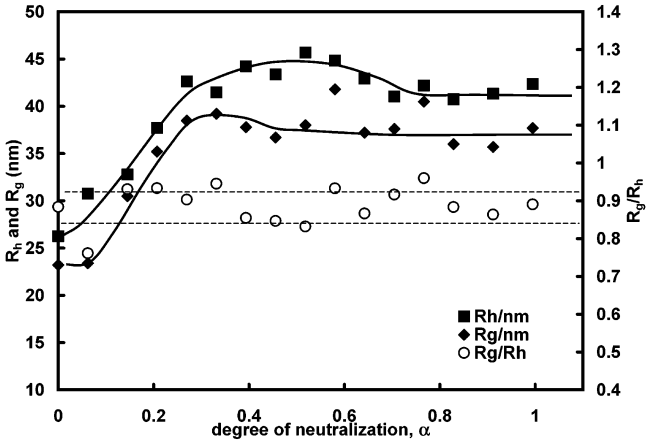

Figure 7. R_h^{app}, R_g^{app}, and $\rho(R_g/R_h)$ of 0.02 wt % P(MAA-*b*-MMA) polymer solution measured at different α: (■) R_h^{app}; (◆) R_g^{app}; (○) ρ (R_g/R_h).

Static Light Scattering. The *z*-average radius of gyration (R_g) of the P(MAA-*b*-MMA) polymer at different α were measured using static light scattering (SLS), and the values were also included in Figure 7. It is found that R_g is lower than R_h over the whole α ranges. However, the dependence of R_g on α resembles that of R_h, where it increases from ~23 to ~38 nm as α increases from 0 to ~0.3 and then it remains unchanged. The parameter ρ (ratio R_g/R_h) can be used to examine the morphology of the microstructure of the micelle. It is found ρ is independent of α and remains essentially constant of 0.88. This value is different from the theoretical ρ values corresponding to the structures of hard sphere, Gaussian chain, and long rod, which are 0.774 (e.g., unneutralized MAA−EA random copolymer), 1.501 (e.g., fully neutralized MAA−EA random copolymer), and ≥2, respectively.[31,32] A vesicle structure is not possible either, because the particle size and the aggregation number (which will be discussed later) are far too low compared to the reported values for vesicle.[10,33]

A ρ of approximately 0.9 characterizing a core−shell structured micelle for polyisobutylene-*b*-poly(methacrylic acid) block copolymers has been reported by Schuch et al.[10] Therefore, it is believed the $\rho = 0.88$ for the P(MAA-*b*-MMA) polymer also corresponds to a micellar structure with a dense MMA core and MAA shell, which is consistent with the result obtained from potentiometric titration. Moreover, comparison of the measured radii of the micelle (∼23 nm before neutralization and ∼38 nm after neutralization) with the contour length of a single polymer chain (∼40 nm) also indicates that a single-layered micellar structure is the most probable microstructure.

It is known that R_g is responsive to the mass distribution of the micelle. The shell layer of MAA blocks mainly contributes to the mass distribution of the micelle because the molar composition of MAA is approximately 91%. With the addition of NaOH, the shell layer expands upon ionization and the size of the micelle increases, represented by the increase of R_g with α. On the other hand, R_h is responsive to the hydrodynamics of the micelle, which includes the contribution from the solvent molecules upon hydration. Hence, R_h is higher than R_g over the entire range of neutralization.

The weight-average molar mass (M_w) of the micelles can be obtained from SLS measurements based on the Debye equation:

$$\frac{KC}{R(q)} = \frac{1}{M_w}\left(1 + \frac{1}{3}R_g{}^2q^2\right) + 2A_2C \qquad (6)$$

where K is an optical parameter ($K = [4\pi^2 n_{tol}{}^2(dn/dc)^2]/N_A\lambda^4$ where n_{tol} is the refractive index of toluene (1.494), dn/dc is the refractive index increment of the polymer measured using BI-DNDC, N_A is Avogadro's constant, and λ is the wavelength), C is the concentration of the polymer solution, $R(q)$ is the Rayleigh ratio, q is the scattering vector, and A_2 is the second virial coefficient. The absolute excess time-averaged scattered intensity, i.e., Rayleigh ratio $R(q)$, is expressed by the equation

$$R(q) = R_{tol,90}\left(\frac{n}{n_{tol}}\right)^2\frac{I - I_0}{I_{tol}}\sin\theta \qquad (7)$$

where $R_{tol,90}$ is the Rayleigh ratio of toluene at scattering angle 90° with a value of 40×10^{-6} cm^{-1}, n is the refractive index of the solvent, I, I_0, and I_{tol} are the scattered intensities of the solution, solvent, and toluene, respectively, and θ is the scattering angle. In our case, the concentration of the polymer solution is sufficiently low (2×10^{-4} g/mL), and the $2A_2C$ term in eq 6 is expected to be negligible. Therefore, the intercept of the plot of $KC/R(q)$ against q^2 yields the inverse of the apparent weight-average molar mass ($M_w{}^{app}$); consequently, the aggregation number of the micelle can be evaluated using the equation $Z = M_w{}^{app}/M_w{}^0$, where $M_w{}^0$ is the molar mass of the single polymer chain. In the present study, $KC/R(q)$ exhibits a linear relationship with q^2 at all degrees of neutralization as depicted in Figure 8. The $M_w{}^{app}$ obtained from the intercepts by linear fitting of the plots shown in Figure 8 is found to be essentially independent of α and has an average value of $2.25 \times 10^5 \pm 2.6 \times 10^4$ g/mol. The average aggregation number, Z, is 20 ± 2 where the molar mass of the single polymer chain is 1.187×10^4 g/mol, determined from GPC measurement. The aggregation number is in good agreement with the aggregation number $Z = 25$ for unneutralized P(MAA-*b*-MMA) micelle as reported by Liu et al.[16] The constant $M_w{}^{app}$, Z, and ρ over the entire range of α indicates that the microstructure of the micelle remains unchanged during neutralization, which coincides with the finding revealed by the potentiometric titration that no conformational transition is observed in the course of titration. The proposed microstructure of the micelle of P(MAA-*b*-MMA) block copolymer is depicted schematically in Figure 9. It is known that the hydrophobic association is an entropy-driven process, where the entropy gain is attributed to the released water molecules from the disrupted solvent cage surrounding the hydrophobes. Consequently, the water structure is significantly affected by the association behavior of the polymer, which drives the micellization behavior of the block copolymer.

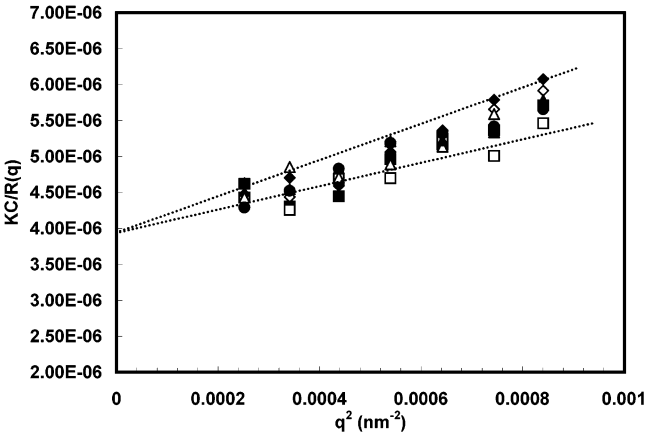

Figure 8. $KC/R(q)$ vs the square of the scattering vector (q^2) for 0.02 wt % P(MAA-*b*-MMA) polymer solution at different degree of neutralization, α [0.06, ◇; 0.20, ■; 0.33, □; 0.44, ◆; 0.56, △; 0.77, ▲; 0.99, ●].

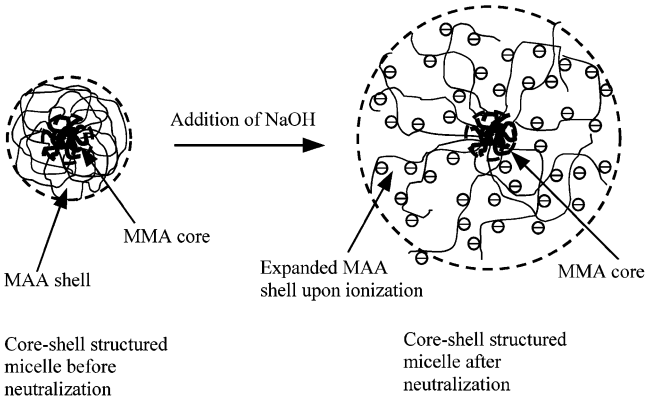

Figure 9. Proposed microstructure of the micelle of the P(MAA-*b*-MMA) block copolymer at different degrees of neutralization.

Conclusions

The micellar structure and the neutralization behavior of the P(MAA-*b*-MMA) copolymer were examined using DLS, SLS, and potentiometric titration. P(MAA-*b*-MMA) polymer exists as spherical micelles consisting of a hydrophobic MMA core surrounded by a hydrophilic MAA shell. The molar mass of the micelle is approximately 2.25×10^5g/mol with an aggregation number ∼20. Both R_h and R_g increase with α (R_h and R_g increase from 26 to 42 nm and from 23 to 38 nm, respectively), characterizing the expansion of the shell layer upon ionization due to neutralization. However,

the ratio R_g/R_h remains constant at 0.88, and the pK_a increases steadily with α, suggesting that the micellar structure remains unchanged in the course of neutralization. This is significantly different from the random MAA−EA copolymers that behave a conformational change during neutralization.

Acknowledgment. R.P. acknowledges the financial support for the postdoctoral fellowship provided by the Singapore-MIT (SMA) Alliance.

References and Notes

(1) Hamley, I. W. *The Physics of Block Copolymers*; Oxford University Press: Oxford, 1998.
(2) Klok, H. A.; Lecommandoux, S. *Adv. Mater.* **2001**, *13*, 1217.
(3) Winnik, M. A.; Yekta, A. *Curr. Opin. Colloid Interface Sci.* **1997**, *2*, 424.
(4) Urban, D.; Gerst, M.; Rossmanith, P.; Schuch, H. *Polym. Mater. Sci. Eng.* **1998**, *79*, 440.
(5) Sukhorukov, G. B.; Antipov, A. A.; Voigt, A.; Donath, E.; Mohwald, H. *Macromol. Rapid Commun.* **2001**, *22*, 44.
(6) Sauer, M.; Meier, W. *Chem. Commun.* **2001**, *1*, 55.
(7) Zhang, X.; Matyjaszewski, K. *Macromolecules* **1999**, *32*, 1763.
(8) Zhang, L. H.; Eisenberg, A. *Science* **1995**, *268*, 1728.
(9) Zhang, L. H.; Barlow, R. J.; Eisenberg, A. *Macromolecules* **1995**, *28*, 7135.
(10) Schuch, H.; Klingler, J.; Rossmanith, P.; Frechen, T.; Gerst, M.; Feldthusen, J.; Müller, A. H. E. *Macromolecules* **2000**, *33*, 1734.
(11) Stepanec, M.; Podhajecka, K.; Tesarova, E.; Prochazka, K.; Tuzar, Z.; Brown, W. *Langmuir* **2001**, *17*, 4240.
(12) Gohy, J. F.; Willet, N.; Varshney, S.; Zhang, J. X.; Jerome, R. *Angew. Chem., Int. Ed.* **2001**, *40*, 3214.
(13) (a) Kriz, J.; Masar, B.; Plestil, J.; Tuzar, Z.; Pospisil, H.; Doskocilova, D. *Macromolecules* **1998**, *31*, 41. (b) Kriz, J.; Plestil, J.; Tuzar, Z.; Pospisil, H.; Brus, J.; Jakes, J.; Masar, B.; Vlcek, P.; Doskocilova, D. *Macromolecules* **1999**, *32*, 397.
(14) Talingting, M. R.; Munk, P.; Webber, S. E.; Tuzar, Z. *Macromolecules* **1999**, *32*, 1593.
(15) Kriz, J.; Masar, B.; Pospisil, H.; Plestil, J.; Tuzar, Z.; Kiselev, M. A. *Macromolecules* **1996**, *29*, 7853.
(16) Liu, T.; Schuch, H.; Gerst, M.; Chu, B. *Macromolecules* **1999**, *32*, 6031.
(17) Kriz, J.; Kurkova, D.; Kadlec, P.; Tuzar, Z.; Plestil, J. *Macromolecules* **2000**, *33*, 1978.
(18) (a) Cao, T.; Munk, P.; Ramireddy, C.; Tuzar, Z.; Webber, S. E. *Macromolecules* **1991**, *24*, 6300. (b) Prochazka, K.; Kiserow, D.; Ramireddy, C.; Tuzar, Z.; Munk, P.; Webber, S. E. *Macromolecules* **1992**, *25*, 454.
(19) Zhang, X.; Xia, J.; Matyjaszewski, K. *Polym Prepr (Am. Chem. Soc., Div. Polym. Chem.)* **1999**, *40* (2), 440.
(20) Shipp, D. A.; Wang, J. L.; Matyjaszewski, K. *Macromolecules* **1998**, *31*, 8005.
(21) Davis, K. A.; Matyjaszewski, K. *Macromolecules* **2000**, *33*, 4039.
(22) Wang, C.; Tam, K. C.; Jenkins, R. D.; Bassett, D. R. *Phys. Chem. Chem. Phys.* **2000**, *2*, 1967.
(23) Wang, C.; Tam, K. C.; Jenkins, R. D. *J. Phys. Chem. B* **2002**, *106*, 1195.
(24) Ochiai, H.; Anabuki, Y.; Kojima, O.; Tominaga, K.; Murakami, I. *J. Polym. Sci., Part B: Polym. Phys.* **1990**, *28*, 233.
(25) Leyte, J. C.; Mandel, M. *J. Polym. Sci.* **1964**, *2*, 1879.
(26) Mandel, M.; Leyte, J. C. *J. Electroanal. Chem.* **1972**, *33*, 297.
(27) Barone, G.; Virgilio, N. D.; Elia, V.; Rizzo, E. *J. Polym. Sci.* **1974**, *44*, 1.
(28) Dubin, P.; Strauss, U. P. *J. Phys. Chem.* **1970**, *74*, 2842.
(29) Dubin, P.; Strauss, U. P. *J. Phys. Chem.* **1973**, *77*, 1427.
(30) Hermans, J., Jr. *J. Phys. Chem.* **1966**, *70*, 510.
(31) Wu, P.; Mohammad, S.; Chen, H.; Qiang, D.; Wu, C. *Macromolecules* **1996**, *29*, 277.
(32) Förster, S.; Hermsdorf, N.; Böttcher, C.; Linder, P. *Macromolecules* **2002**, *35*, 4096.
(33) Chécot, F.; Lecommandox, S.; Gnanou, Y.; Klok, H. *Angew. Chem., Int. Ed.* **2002**, *41*, 1339.

MA021302J